Exploiting the flexibility potential of water distribution networks: A pilot project in Belgium

Ioannis Boukas*, Elodie Burtin†, Antonio Sutera†, Quentin Gemine†, Bernard Pevee‡, and Damien Ernst*§
* Department of Electrical Engineering and Computer Science, University of Liège, Liège, Belgium,
†Intelligent Systems Solutions, Haulogy, Liège, Belgium
‡Société wallonne des eaux, Liège, Belgium,
§LTCI, Telecom Paris, Institut Polytechnique de Paris, Paris, France

***Abstract*—Flexibility, and in particular, energy storage is expected to assume a key role in the efficient and secure operation of the power system, and thus, in the transition towards a carbon-free electricity sector. In this paper, we propose a methodology for exploiting the flexibility existing in water distribution systems from water storage in reservoirs. The methodology relies first on a modelling approach, from which an optimization problem is defined. The resolution of this optimization problem leads to an operating pattern for the pumps. The methodology assumes that all the electricity is bought on the day-ahead market, where the bids are placed by constructing and solving an optimization problem. The uncertain water consumption and the electricity market prices are predicted using machine learning techniques. The methodology is tested on a real-life water distribution network in Belgium and the results from the pilot project indicate a cost reduction up to 11%.**

***Index Terms*—Flexibility, Water distribution network, model predictive control**

I. Introduction

Recent directives and goals in Europe and worldwide for decarbonisation of the energy sector have resulted in targets for massive renewable energy sources (RES) integration in the coming decades [1], [2]. This large-scale RES integration however entails risks for the secure operation of power systems. The uncertainty induced by RES due to the inability to predict accurately its power production is expected to lead to substantial challenges on handling imbalances in real-time. Flexibility is essential for achieving effectively the set goals for decarbonisation [3]. In particular, the use of flexibility can assist in shifting energy from times that it is produced to times that it is needed to be consumed [4]. In this way, the matching of supply and demand of electricity can be realised more effectively.

In this paper, we consider the case where flexibility is offered by a large consumer that operates a water distribution network (WDN). Typically, during the operation of a WDN, the water pumps are the most energy intensive components. These pumps are responsible for transferring water between water reservoirs. The flexibility potential lies on the ability to exploit the storage capacity of the reservoirs in a way that allows for scheduling the water pumps in the most cost-effective manner. In particular, we focus on the flexibility that can be exploited in the case of a water treatment station (WTS). In the case of a WTS, the pumping process responsible for transferring water from the production reservoirs to the reservoirs that supply the water demand takes up a large share of the total electricity consumed. In this case, flexibility can be offered by such a station by shifting the pumping processes in time, thus benefiting from the capacity of the existing water reservoirs. This shift leads to effectively placing large parts of the electrical consumption of the station during periods of the day that the electricity is cheaper or when there is excess of local renewable energy production. In this way, the total electricity cost for the station is reduced and the system is operated in a more efficient way.

However, in order to properly be rewarded for its flexibility it is necessary for the WTS operator to have access to an appropriate market mechanism/structure [5]. An appropriate market mechanism is such that provides a temporal granularity that matches with the size of the reservoirs and the pumping capacity of the WTS. In this paper, we consider that the WTS has access to all relevant energy markets through its retailer via a special contract (FLEXI-PROFILE). More specifically, the participation of the WTS operator in the markets is divided in three steps:

1) **Forward:** Reservation of a fixed amount of energy for the target year in the forward markets. Purchasing 1 MW of product CAL 2023 corresponds to a block of energy purchase for the year 2023, i.e. 8760 MWh. Forward markets are used by energy market players as a hedge against the risk/volatility/uncertainty of the spot markets, i.e. the day-ahead market. The price at which energy is traded in the long-term markets is said to be an expectation of what the average day-ahead market price will be for the given period.
2) **Day-ahead:** Nomination of the amount of energy that will be consumed by the WTS during each quarter-hour of the next day. In Europe the day-ahead market is cleared around midday one day in advance and energy exchanges take place in hourly time-slots. Although, there is one energy price per hour the retailer requests for a quarter-hourly nomination in order to manage the imbalance settlement process.
3) **Imbalance settlement:** The difference between the market position (forward and day-ahead) of the WTS operator and the real/measured consumption for each

quarter of the day is penalised by the imbalance price.

In this paper, we focus on addressing the short-term energy management of the WTS. To this end, for the sake of simplicity, in the presented methodology, we do not consider at all the forward step. More precisely, we consider that there is no energy reserved in the forward market. We also assume that the WTS operator does not intend to arbitrage between the day-ahead market and the imbalance market by speculating on the price difference between the two markets. This is a reasonable assumption that is made to reduce the risk/exposure of the WTS since its core business is not energy trading but water production. Additionally, the WTS operator in real-time is assumed to perform all means necessary to avoid any imbalances between the nominated and the realized energy consumption regardless of the imbalance prices.

Broadly speaking, the participation of consumers in the electricity markets, in the context of demand-side management (DSM) or demand-side response (DSR), for the procurement of flexibility has been extensively studied in the literature [6], [7]. An optimal bidding strategy for the participation of a variety of flexible demand-side resources (e.g. plug-in electric vehicles and distributed generation and flexible load) in the day-ahead market is proposed in [8], [9]. The authors consider explicitly the uncertainties related to the market price, the renewable generation and the electrical consumption and solve the problem by constructing robust optimization model that accounts for risk. Similarly, the strategic participation of flexible loads in air-conditioned buildings is proposed in [10]. A detailed model of the building is used to capture the relationship between the occupant comfort and the electrical consumption for heating, ventilation, and air-conditioning (HVAC). The optimal bidding strategy and real-time control of the system is determined using model-predictive control (MPC).

Beyond traditional DSM technologies, the coupling of the WDN with the power system for flexibility procurement has been proposed recently in the literature [11], [12]. In [13], [14] the optimal water flow problem is formulated accounting for the WDN topology and the hydraulic constraints imposed by each component (e.g. water pumps, junctions, tanks, reservoirs). The originally formulated optimization problem is nonconvex and is subsequently approximated using convex relaxations. A key assumption for constructing this model is that we have full knowledge of all the network parameters. In practice, this task becomes increasingly complex as the size of the WDN grows. Moreover, the participation of a WDN in DSR and in particular in offering grid services is investigated in [15], [16]. In [15] the hydraulic constraints of each component are modeled explicitly and a linearization method is employed to reduce the computation time needed, while price and water demand uncertainty is not considered. Results demonstrate promising profit opportunities for water distribution system operators both in DSR and frequency regulation markets, by co-optimizing the schedule of water pumps and tanks over the whole network. In [16], flexibility is offered by a WDN operator in order to procure both voltage support and frequency regulation to the grid.

The participation of a WDN in the French wholesale energy market through a specific mechanism ("Notification d'Echange de Blocs d'Effacement" (NEBEF)) is investigated in [17]. The novelty introduced by the proposed approach is related to the management of the uncertainty stemming from water consumption in the network. In order to account for the water demand uncertainty a chance constrained problem is formulated to integrate water systems flexibility to power system operation. A similar approach is followed in [18], where a chance-constrained optimization framework is used to account for water demand uncertainty. Results indicate that the approach is conservative leading to high reliability at high cost. A machine learning approach is proposed in [19] for predicting the water consumption. The forecasts are then used to control water pumps with the goal to smoothen the electricity consumption and to shave peaks in a remote island in Greece. Results indicate gains up to 15%.

In this paper, we focus on deriving an optimal bidding strategy and an optimal real-time control for the operation of an individual WTS instead of the entire WDN. However, the proposed modeling framework can be extended to the case where there is a set of WTS that need to be co-optimized. Moreover, we implement the proposed approach on a real WTS located in Belgium and we report results collected during the pilot phase. In the following, we frame the problem of a WTS operator maximizing the value of flexibility in the short-term markets as following. Firstly, the WTS operator needs to predict the day-ahead market prices, the uncontrollable water flows (i.e. water demand) and the uncontrollable power consumption of the WTS for the following day. Based on these predictions and a model of the WTS, an optimal day-ahead plan is constructed and is nominated to the retailer. This plan is created by optimizing the operation of the pumping processes and the utilisation of the water reservoirs in such a way that the total cost of energy is minimized while respecting any operating constraints related to the security of water supply, protection of equipment, etc. Secondly, once the day-ahead plan is nominated the real-time controller is responsible for matching the nominated day-ahead plan to the real-time consumption of the WTS.

II. Problem description

In this section, we describe in detail the market participation of a WTS operator. First, we present the decision-making process of the operator in the short-term markets. Subsequently, we describe the discrete time model used for modelling the operation of a generic WTS.

A. Water treatment station operation

In this section, we present an abstract framework that is used to model the operation of a WTS. A schematic of the generic representation of a WTS is illustrated in Figure 1. This framework together with data from a real WTS is used to have a concrete representation of each individual WTS that is controlled. There are two main building blocks in this generic

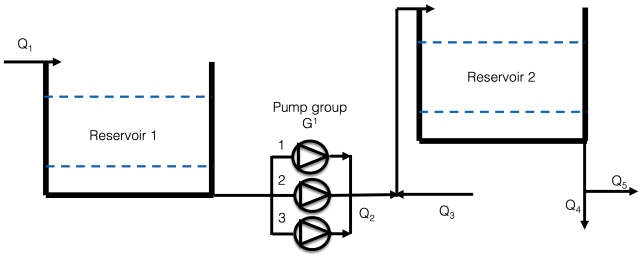

Fig. 1: Schematic of a generic water treatment station. Reservoirs are connected with water flows that can be controllable by a set of pumps or uncontrollable (e.g. water consumption).

WTS model, namely the **reservoirs** and the **water flows** that enter in or exit from the reservoirs.

1) Water flows: Let $Q_{i,t}[m^3/h]$ denote the i-th flow of water at time step t in the set of water flows $\mathbb{Q}$ considered, with $i \in \mathbb{Q} = \{1, 2, .., I\}$. Water flows are categorised in two subsets, namely controllable $\mathbb{Q}^c \subseteq \mathbb{Q}$ and uncontrollable $\mathbb{Q}^u \subseteq \mathbb{Q}$. For instance, as shown in Figure 1, flows Q_1, Q_3, Q_4, Q_5 are considered to be uncontrollable whereas flow Q_2 is considered to be controllable.

Each controllable flow $Q_{i,t}$ are effectively controlled by a group/set of pumps $\mathbb{G}^i$. The pumps considered in this analysis are assumed to be driven by a fixed speed motor. Each pump $g \in \mathbb{G}^i$ is considered to have a nominal power consumption $\bar{P}^g$ and a nominal flow $\bar{Q}^g$, with $g \in \{1, 2, ...\} \subset \mathbb{N}$. Additionally, each pump is considered to have a binary status $s_t^g \in \{0, 1\}$ that takes the value 0 when the pump is off and the value 1 when the pump is on at each time step t. Additionally, we consider a number of periods k during which each pump needs to remain on once it is activated and a number of periods m during which each pump needs to remain off once it is deactivated. This allows for limiting the number of activations and deactivations that could potentially lead to degradation of the pump or its motor. For example, in the presented Figure 1, pump group $\mathbb{G}^1$ is used to control flow Q_2 and is composed of three pumps namely $g \in \{1, 2, 3\}$.

At each time step t the water flow $Q_{i,t}$ for each controllable flow $i \in \mathbb{Q}^c$ can be computed as a function of the status of each pump in the pump group $\mathbb{G}^i$ according to:

$$Q_{i,t} = \sum_{g \in \mathbb{G}^i} s_t^g \cdot \bar{Q}^g \tag{1}$$

At each time step t the power consumption $P_{i,t}$ that corresponds to controllable water flow $i \in \mathbb{Q}^c$ can be computed accordingly as:

$$P_{i,t} = \sum_{g \in \mathbb{G}^i} s_t^g \cdot \bar{P}^g \tag{2}$$

The total electrical consumption of the WTS P_t at each time step t is given by the sum of the controllable power, the uncontrollable power consumption of the station P_t^{upc} and the renewable energy sources (e.g. solar photovoltaic etc.) generation P_t^{res} as:

$$P_t = \sum_{i \in \mathbb{Q}^c} P_{i,t} + P_t^{upc} - P_t^{res} \tag{3}$$

The term uncontrollable power consumption P_t^{upc} is used to denote the set of electrical devices in the WTS such as electrical motors related to water filtering etc. over which we do not have any control.

The set of uncontrollable flows $\mathbb{Q}^u$ corresponds to processes that are not controlled by the operator such as the water demand of the area or the cleaning of the water filters (which is a seasonal operation that cannot be interrupted). These processes will be modelled by means of statistical models, as described in Section III.

2) Reservoirs: Let SoC_t^r denote the state of charge of the reservoir $r \in \{1, 2, ..., R\} \subset \mathbb{N}$ time step t, with $SoC_t^r[m^3] \in \left[\underline{SoC}^r, \overline{SoC}^r\right]$. It is considered that a set of inflows $\mathbb{Q}^{r,in} \subseteq \mathbb{Q}$ and outflows $\mathbb{Q}^{r,out} \subseteq \mathbb{Q}$ are attached to each reservoir r. For instance, in Figure 1, for reservoir 1 it is considered that $\mathbb{Q}^{1,in} = \{Q_1\}$ and $\mathbb{Q}^{1,out} = \{Q_2\}$, while for reservoir 2 we have $\mathbb{Q}^{2,in} = \{Q_2, Q_3\}$ and $\mathbb{Q}^{2,out} = \{Q_4, Q_5\}$. More formally, we can define an adjacency matrix with dimension $R \times I$ for grouping together all the inflows and outflows for all reservoirs.

$$A = \begin{bmatrix} a_{11} & a_{12} & \cdots & a_{1I} \\ a_{21} & a_{22} & \cdots & a_{2I} \\ \vdots & \vdots & \ddots & \vdots \\ a_{R1} & a_{R2} & \cdots & a_{RI} \end{bmatrix} \tag{4}$$

Each element $a_{r,i}$ takes values in $\{-1, 0, 1\}$ depending on whether flow Q_i is an outflow, not connected or an inflow to reservoir r respectively.

We can also define the efficiency matrix η with dimensions $R \times I$ that represents the losses/leakages for each inflow/outflow as:

$$\eta = \begin{bmatrix} \eta_{11} & \eta_{12} & \cdots & \eta_{1I} \\ \eta_{21} & \eta_{22} & \cdots & \eta_{2I} \\ \vdots & \vdots & \ddots & \vdots \\ \eta_{R1} & \eta_{R2} & \cdots & \eta_{RI} \end{bmatrix} \tag{5}$$

Parameters $\eta_{r,i}$ represent the losses/leakages for each inflow/outflow i for reservoir r. Parameters $\eta_{r,i}$ take values $\eta_{r,i} \geq 1$ when dealing with outflows and values $\eta_{r,i} \leq 1$ when dealing with inflows. Appropriate values for these parameters can identified by performing a system identification process using data from the WTS that we intend to model. This process is described in detail in Section III.

Let Q_t denote the vector containing all the flows at timestep t, defined as:

$$Q_t = \begin{bmatrix} Q_{1,t} & Q_{2,t} & \cdots & Q_{I,t} \end{bmatrix} \tag{6}$$

The state of charge matrix SoC_t can be defined as:

$$SoC_t = \begin{bmatrix} SoC_t^1 & SoC_t^2 & \cdots & SoC_t^R \end{bmatrix} \tag{7}$$

The evolution of the state of charge in matrix notation is given by:

$$SoC_{t+\Delta t} = SoC_t + A \odot \eta \cdot Q_t^T \tag{8}$$

The symbol $\odot$ is used to denote the Hadamard product, also known as the element-wise product.

B. Market participation

Let us consider a flexible WTS operator nominating its consumption for the next day in the day-ahead market and controls in real-time the consumption of the station.

The decision timeline for the flexible WTS for a day D is presented in Figure 2. At each time step $t \in T = \{00:00, ..., 23:45\}$ the WTS operator takes decisions about the level of the real-time consumption P_t. The real-time consumption of the WTS is defined in Section II-A1. For the sake of simplicity regarding the notation and the indexing, we will assume that the decision timeline and the actual delivery of power have the same interval i.e. $\Delta t = 15min$.

In addition to that, one day in advance $(D-1)$ at 10 a.m. the WTS operator nominates/submits in the day-ahead market the 96 values of its net consumption profile for the next day (D). More formally, the WTS operator decides the day-ahead profile for day D, denoted by $P_D^{DA} = \left\{P_t^{DA}, \quad \forall t \in T\right\}$. When the day-ahead market clears, the prices for each hour of the next day $\lambda_D^{DA} = \left\{\lambda_t^{DA}, \quad \forall t \in T\right\}$ become known. While in reality the day-ahead prices have an hourly granularity, in the FLEXI-PROFILE contract its specified that the WTS operator nominates quarter-hourly profiles. Therefore, we assume the day-ahead prices to be at a constant level for each quarter of the same hour. It is stipulated by the contract, that if the day-ahead nominated power is positive the WTS buys its energy at the day-ahead market price, whereas if the day-ahead nominated power is negative (production), the WTS sells energy to the market at a fixed contractually predefined price λ^{Sell}, that does not depend on the time.

The WTS operator can compute its day-ahead cost at each timestep $t \in T$ as:

$$C_t^{DA} = \begin{cases} \lambda_t^{DA} \cdot |P_t^{DA}|, & \text{if} \quad P_t^{DA} \geq 0., \\ -\lambda^{Sell} \cdot |P_t^{DA}|, & \text{otherwise.} \end{cases} \tag{9}$$

The imbalance P_t^{IM} at each timestep t is defined as:

$$P_t^{IM} = P_t - P_t^{DA}, \tag{10}$$

The imbalance price λ_t^{IM} for each quarter becomes known at the end of the quarter. The imbalance cost can be computed as:

$$C_t^{IM} = \lambda_t^{IM} \cdot P_t^{IM}, \tag{11}$$

As described in Section I, in this paper we assume that the WTS operator does not intend to arbitrage between the day-ahead market and the imbalance market by speculating on the price difference between the two markets. Additionally, in real-time, the operator could deviate its consumption from the day-ahead plan in order to benefit from the imbalance prices. However, this would imply that the WTS operator has access to accurate forecasts of the imbalance price. This can be very risky because imbalance markets are highly volatile. Instead, at each timestep t in real-time the WTS operator controls its consumption in order to match its day-ahead nomination while satisfying the operational constraints of the unit.

C. Problem definition

In this section, we define the problem faced by a WTS operator that participates in the day-ahead market. The cost minimization objective for electricity transacted in the day-ahead market faced by a WTS operator can be summarized as:

$$\min_{\{P_t, P_t^{DA}, \forall t \in T\}} \sum_{t \in T} \lambda_t^{DA} \cdot P_t^{buy} - \lambda^{sell} \cdot P_t^{sell} \tag{12}$$

where at each timestep we ensure that the power consumption/production P_t is bought/sold in the market. Thus, we have:

$$P_t = P_t^{DA} \tag{13}$$

$$P_t^{DA} = P_t^{buy} - P_t^{sell} \tag{14}$$

$$P_t^{buy}, P_t^{sell} \geq 0 \tag{15}$$

The solution of this optimization model yields the optimal day-ahead nomination plan and the optimal real-time power consumption for the WTS. However, in reality, the day-ahead nomination problem cannot be solved optimally due to the various sources of uncertainty at the day-ahead stage. More specifically, at the day-ahead decision stage there is uncertainty related to the day-ahead prices (λ_t^{DA}), the uncontrollable water flows ($Q_{i,t}, \quad \forall i \in \mathbb{Q}^u$), the uncontrollable power consumption (P_t^{upc}) and the renewable power generation (P_t^{res}).

The uncertainty related to the the uncontrollable water flows, the uncontrollable power consumption and the renewable power generation may result in discrepancies between the real-time consumption and the day-ahead plan. Therefore, during real-time operation, the WTS operator needs to solve an optimization problem with the objective to minimimize deviations (ΔP_t^{up}, ΔP_t^{down}) from the day-ahead plan according to:

$$\min_{\{P_t \forall t \in T\}} \sum_{t \in T} C \cdot (\Delta P_t^{up} + \Delta P_t^{down}), \tag{16}$$

where we have:

$$P_t = P_t^{DA} + \Delta P_t^{up} - \Delta P_t^{down} \tag{17}$$

$$\Delta P_t^{up}, \Delta P_t^{down} \geq 0 \tag{18}$$

The objective presented in equation (16) aims at penalizing by a factor C any deviations (ΔP_t^{up}, ΔP_t^{down}) between the real-time consumption of the WTS P_t and the day-ahead nominated schedule P_t^{DA}. At the real-time stage uncertainty is mostly related to the uncontrollable water flows. In the following we develop a methodology that creates forecasts of the various sources of uncertainty. Moreover, we decouple the optimization problem in two distinct models. One that is

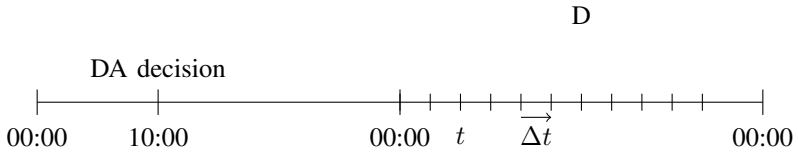

Fig. 2: Decision timeline for day-ahead nomination and real-time control.

solved at the day-ahead stage and one that is solved in real-time at each timestep t in order to correct any discrepancies between the predicted and the realized plan. The methodology for generating predictions for the uncertain variables, as well as, the optimization models solved for taking optimal decisions in day-ahead and real-time are presented in the following section.

III. Methodology

As detailed in Section II, the decision making problem of a flexible WTS operator participating in the short-term markets consists in two stages, namely i) the day-ahead nomination of the amount of energy that will be consumed during each quarter of the next day and ii) the real-time control of the controllable flows. In this section, we describe the methodology used for solving the aforementioned problem. We first describe the methodology used to estimate the parameters of the WTS through a system identification process that relies on historical data. Subsequently we describe the methods used to create predictions of the prices, the uncontrollable flows and the residual consumption at the day-ahead stage. We proceed by presenting the optimization model used at the day-ahead stage to determine the optimal power nomination. Finally, we present the optimization model that is solved during real-time in order to generate the optimal control of the pumps that matches the nominated day-ahead plan.

A. System identification

As described in Section II-A2, in order to have a realistic model for estimating the state of charge for reservoir $r \in R$ at each time step t, the values of the efficiency parameters η need to be identified. To achieve that, we use the model presented in equation (8) and historical data regarding the matrices of the flows Q_t and the state of charge of the reservoirs SoC_t. The historical dataset containing H sequential data samples can be defined as:

$$B = \{\{\tilde{SoC}_0, \tilde{SoC}_1, \cdots, \tilde{SoC}_H\}, \{\tilde{Q}_0, \tilde{Q}_1, \cdots, \tilde{Q}_H\}\}.$$

We use each sample $\tilde{SoC}_h, \tilde{Q}_h$ in the historical dataset and the model presented in equation (8) to produce estimates of the state of charge matrix $\hat{SoC}_{h+1}$ at the next timestep. Subsequently, we aim at finding the parameters η that minimize the error between the estimates of the model $\hat{SoC}_{h+1}$ of equation (8) and the historical data $\tilde{SoC}_{h+1}$. We have:

$$\eta = \arg\min_{\eta} \frac{1}{H} \sum_{h \in \{1,\cdots,H\}} (\hat{SoC}_h - \tilde{SoC}_h)^2 \quad (19)$$

$$s.t. \quad \hat{SoC}_{h+1} = \tilde{SoC}_h + A \odot \eta \cdot \tilde{Q}_h^T, \quad \forall h \in \{0, \cdots, H-1\}. \quad (20)$$

B. Day-ahead price forecasting

The WTS operator every day D at 10 a.m. needs to nominate the power that will be consumed for the operational needs of the WTS during the next day. The WTS operator schedules most of its consumption during periods of the day that the price of electricity is at the lowest levels. To identify these periods of the day the WTS operator creates predictions of the day-ahead price for the following N days. We define the look-ahead horizon at day D that is denoted by $\bar{T} = \{D \quad 00:00, D \quad 00:15..., D+N \quad 23:45\}$. We denote as $\hat{\lambda}_D^{DA} = \left\{\hat{\lambda}_t^{DA}, \quad t \in \bar{T}\right\}$, the forecast of the day-ahead market prices for the the following N days.

In order to generate predictions for the day-ahead prices of the following days we use an auto-regressive time-series model $pred_{DA}$ that relies on historical values of the day-ahead price of the past M days. We denote as λ_{D-1}^{DA} the 96 quarter-hourly values of the day-ahead price for day $D-1$. The prediction task can be described by:

$$\hat{\lambda}_D^{DA} = pred_{DA}(\lambda_{D-1}^{DA}, ..., \lambda_{D-M}^{DA}) \quad (21)$$

More specifically, the model $pred_{DA}$ is an instance of *Facebook Prophet*, that is a decomposition time-series framework that decomposes the signal in its trend, its seasonality and the holidays [20]. The parameters of the model $pred_{DA}$ are tuned using a large dataset of historical values of the day-ahead prices.

The motivation behind using such a model lies on the fact that the day-ahead price formation depends on the strong daily seasonality of the electricity demand. In addition to that, in this particular application, we are not necessarily interested to obtain high accuracy on the precise value of the prediction of the absolute day-ahead price. Instead, we are more interested in predicting the spread and the time periods of peak versus off-peak prices, because this information is in essence what will lead the WTS to schedule its controllable consumption.

C. Uncontrollable water flow forecasting

There are two different types of flows that can be considered uncontrollable in the context of a WTS. The first type refers

to flows that correspond to water demand from the users. The latter corresponds to water inflows/outflows that originate from or are directed towards some internal process of the station e.g. water production, filter cleaning etc.

For the prediction task of the first type of uncontrollable water flows that corresponds to user water demand we use an auto-regressive seasonality model. The motivation behind the use of such a model lies on the fact that generally speaking, the water demand has strong daily and yearly seasonality components. To this end, we denote the forecast of the uncontrollable seasonal flows as $\hat{Q}_{i,D} = \left\{\hat{Q}_{i,t}, \quad t \in \bar{T}\right\}$, where $i \in \mathbb{Q}^u$. Similar to the day-ahead forecasting process we define a water flow forecasting model $pred_Q$ that relies on the historical realizations of the uncontrollable flow of the past M days as:

$$\hat{Q}_{i,D} = pred_Q(Q_{i,D-1}, ..., Q_{i,D-M}) \tag{22}$$

The parameters of the model $pred_Q$ are tuned using a large dataset of historical values of each flow Q_i. We denote as $Q_{i,D-1}$ the 96 quarter-hourly values of the flow for day $D-1$.

For the prediction task of the second type of uncontrollable water flows a detailed analysis on the nature of the process is necessary. Depending on the underlying physical task, a custom model can be constructed in order to predict its values for the considered look-ahead horizon. For the case study presented in this paper, the methodology for tackling the prediction task of these flows is detailed in Section IV-C. However, there is no generic methodology that can be abstracted and used in every setting and it is therefore case-sensitive.

D. Uncontrollable consumption & RES generation forecasting

As described in Section II-A1, the uncontrollable power consumption consists of any uncontrollable processes at the WTS that consume electrical power. The prediction of the uncontrollable consumption denoted as $\hat{P}_D^{upc,DA} = \left\{\hat{P}_t^{upc} \quad t \in \bar{T}\right\}$. The prediction of the renewable generation is denoted as $\hat{P}_D^{res,DA} = \left\{\hat{P}_t^{res} \quad t \in \bar{T}\right\}$. The prediction of both the uncontrollable power consumption and the RES generation is also performed by means of an auto-regressive model similar to the two previous prediction tasks presented in equations (21) and (22).

E. Day-ahead optimization model

As described previously, the WTS operator every day at 10 a.m. nominates the consumption level for each quarter of the next day D, denoted by $P_D^{DA} = \left\{P_t^{DA}, \quad \forall t \in T\right\}$. As described in Section II-A1, the day-ahead nomination for the consumption at each time step t of the next day can be split into two parts, namely the day-ahead estimate of the controllable consumption and the forecasts of the uncontrollable part and the RES generation as:

$$P_t^{DA} = \hat{P}_t^{upc} - \hat{P}_t^{res} + \sum_{i \in \mathbb{Q}^c} P_{i,t}.$$

In order to construct its nomination, the WTS operator solves an optimization model to determine the optimal controllable consumption plan. After the system identification and the prediction steps described above, the flexible WTS operator constructs the optimization model as shown in Algorithm 1 for determining the controllable part

$$\left\{\sum_{i \in \mathbb{Q}^c} P_{i,t}, \quad \forall t \in T\right\}$$

of the day-ahead nomination that is submitted each day D to the retailer.

It is important to note that, equations (30) - (34) are used to model the minimum time on/off constraints for protecting the pumps from frequent activations and deactivations. More specifically, binary variables b_t^g and e_t^g are used to indicate whether pump g is activated or deactivated at timestep t respectively. Equation (31) denotes that if pump g was activated at timestep t, i.e. $b_t^g = 1$, it cannot be deactivated in the following k timesteps, i.e. $e_t^g = e_{t+\Delta t}^g = \cdots = e_{t+k\Delta t}^g = 0$. Similarly, equation (32) denotes that if pump g was deactivated at timestep t, i.e. $e_t^g = 1$, it cannot be activated in the following m timesteps, i.e. $b_t^g = b_{t+\Delta t}^g = \cdots = b_{t+k\Delta t}^g = 0$. Additionally, equation (33) imposes a specific order with which pumps are activated in a group of pumps. This constraint is introduced by the technical operation of the WTS. More specifically, the control action transmitted to the operating system of the WTS is the total number of pumps that should be active. The decision about which pumps will be active at each point is a decision made by the operators.

After solving the optimization problem described, we obtain a day-ahead estimate of the values of the flows ($\{Q_{i,D}\}_{i \in \mathbb{Q}^c}$) and the state of charge of the reservoirs ($\{SoC_D^r\}_{r \in R}$). A little subtlety regarding the look-ahead horizon versus the actual day-ahead nomination horizon is that since we are considering the control of water reservoirs it is important to consider a look-ahead horizon longer than one day. The reason for that is that at the end of the horizon the state of the reservoirs would end up at the minimum allowed level. To avoid that we instead consider a longer than one day look-ahead horizon and we only keep for the day-ahead nomination only the results we obtained for the following day.

F. Real-time optimization model

As described previously, after the day-ahead plan is nominated P_D^{DA}, the WTS operator is responsible to control the real-time controllable consumption in such a way that it follows as close as possible the day-ahead plan. To achieve that, the operator would generate new forecasts in real-time for the uncontrollable water flows as described above. The look-ahead horizon for the real-time decision is defined as $\tilde{T}(t) = \{t, ..., t+K \cdot \Delta t\}$. Based on these updated forecasts that depend on the realization of the flows close to real-time, the operator solves the optimization model described in Algorithm 2. The output of this optimization model is the activation or deactivation of the pumps $\{s_t^g, \forall g \in \mathbb{G}^i, \forall i \in \mathbb{Q}^c\}$ considered

This article has been accepted for publication in IEEE Transactions on Smart Grid. This is the author's version which has not been fully edited and content may change prior to final publication. Citation information: DOI 10.1109/TSG.2023.3272469

Algorithm 1: Day-ahead optimization model.

Input: $\bar{T}$: look-ahead horizon,
$\hat{\lambda}_D^{DA}$: day-ahead price forecast,
$\{\hat{Q}_{i,D}\}_{i\in\mathbb{Q}^u}$: uncontrollable water flows forecast,
$\{\bar{P}^g\}_{g\in\{\mathbb{G}^i\}_{i\in\mathbb{Q}^c}}$: nominal power for all pumps,
$\{\bar{Q}^g\}_{g\in\{\mathbb{G}^i\}_{i\in\mathbb{Q}^c}}$: nominal water flow for all controllable flows,
η: efficiencies matrix,
A: adjacency matrix,
$\underline{SoC}$, $\overline{SoC}$: reservoir lower and upper limits.
Output: P_D^{DA}: day-ahead nomination,
$\{Q_{i,D}\}_{i\in\mathbb{Q}^c}$: controllable flows plan,
$SoC_D\}$: day-ahead plan for the state of charge of all reservoirs,
$\{s_D^g\}_{g\in\{\mathbb{G}^i\}_{i\in\mathbb{Q}^c}}$: day-ahead plan for the status of all pumps
Solve:

$$\min \sum_{t\in\bar{T}} \hat{\lambda}_t^{DA}\cdot\Delta t\cdot P_t^{buy} - \lambda^{sell}\cdot P_t^{sell} \tag{23}$$

s.t. $\forall t\in\bar{T}$:

$$P_t^{DA} = \hat{P}_t^{upc} - \hat{P}_t^{res} + \sum_{i\in\mathbb{Q}^c} P_{i,t} \tag{24}$$

$$P_t^{DA} = P_t^{buy} - P_t^{sell} \tag{25}$$

$$P_{i,t} = \sum_{g\in\mathbb{G}^i} s_t^g\cdot\bar{P}^g, \quad \forall i\in\mathbb{Q}^c \tag{26}$$

$$Q_{i,t} = \sum_{g\in\mathbb{G}^i} s_t^g\cdot\bar{Q}^g, \quad \forall i\in\mathbb{Q}^c \tag{27}$$

$$SoC_{t+\Delta t}^r = SoC_t^r + \sum_{i\in\mathbb{Q}^u} a_{r,i}\cdot\eta_{r,i}\cdot\hat{Q}_{i,t} + \sum_{i\in\mathbb{Q}^c} a_{r,i}\cdot\eta_{r,i}\cdot Q_{i,t} \quad \forall r\in R \tag{28}$$

$$\underline{SoC}^r \le SoC_t^r \le \overline{SoC}^r, \quad \forall r\in R, \tag{29}$$

$$s_t^g - s_{t-1}^g = b_t^g - e_t^g, \forall g\in\mathbb{G}^i, \quad \forall i\in\mathbb{Q}^c \tag{30}$$

$$b_t^g + \sum_{t}^{t+k\cdot\Delta t} e_t^g \le 1, \forall g\in\mathbb{G}^i, \quad \forall i\in\mathbb{Q}^c \tag{31}$$

$$e_t^g + \sum_{t}^{t+m\cdot\Delta t} b_t^g \le 1, \forall g\in\mathbb{G}^i, \quad \forall i\in\mathbb{Q}^c \tag{32}$$

$$s_t^1 \le s_t^2 \le \cdots \le s_t^{|\mathbb{G}^i|}, \quad \forall i\in\mathbb{Q}^c \tag{33}$$

$$s_t^g, b_t^g, e_t^g \in \{0,1\}, \forall g\in\mathbb{G}^i, \quad \forall i\in\mathbb{Q}^c \tag{34}$$

$$P_t^{buy}, P_t^{sell} \ge 0 \tag{35}$$

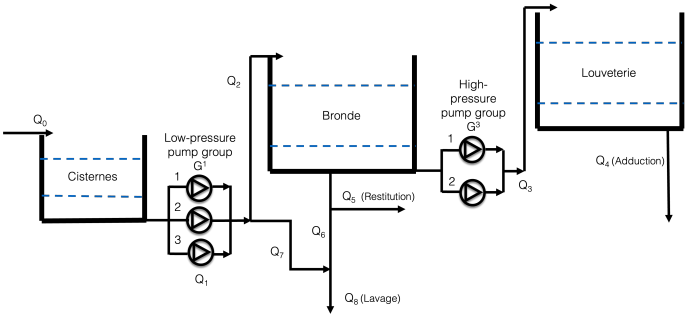

(a) Schematic representation of the Stembert water treatment station.

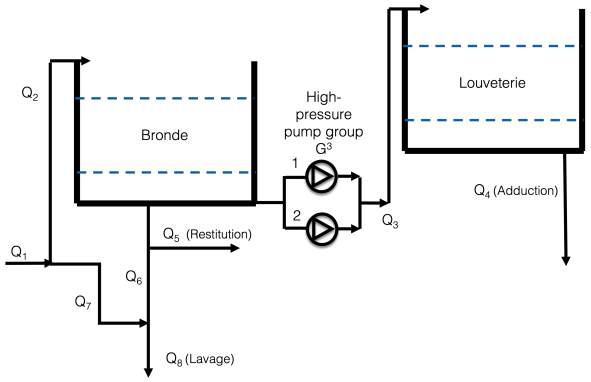

(b) Schematic representation of the subsystem of Stembert water treatment station that is controlled during the pilot phase.

Fig. 3: Schematic representation of Stembert water treatment station.

in order to control optimally the water flows and the electrical consumption of the WTS. While we compute values in the entire look-ahead horizon $\tilde{T}(t)$ only the values computed at time step t are applied to the real system. It is important to note that, similar to the day-ahead problem, equations (42) - (46) are used to ensure the minimum time on/off constraints during the real-time operation as well.

IV. Case Study: Stembert Treatment Station

In the context of a real-life pilot project, the described methodology is used for the day-ahead nomination and real-time control of the Stembert water treatment station located in Verviers, Wallonia, Belgium (50°36'06.6"N 5°54'14.3"E). More specifically, the presented algorithms for the prediction and control of a WTS are implemented in the AMEO[1] (Advance Management of Energy Operations) platform, developed by Haulogy[2]. AMEO allows for data collection and processing from various sources and runs intelligent forecasting and decision-making algorithms to optimize the economic and technical operations of energy systems. AMEO provides advanced monitoring solutions tailored to the considered use case and allows for rapid prototyping and implementation.

[1]https://www.haulogy.net/en/2021/12/17/successful-go-live-in-the-context-of-the-hydroflex-project/

[2]https://haulogy.net/software-platforms/platform-for-new-energy-markets/

Algorithm 2: Real-time optimization model.

Input: $\tilde{T}(t)$: look-ahead horizon,
P_D^{DA}: day-ahead nomination,
C: deviation penalty,
$\{\hat{Q}_{i,\tilde{T}(t)}\}_{i\in\mathbb{Q}^u}$: uncontrollable water flows forecast,
$\{\bar{P}^g\}_{g\in\{\mathbb{G}^i\}_{i\in\mathbb{Q}^c}}$: nominal power for all pumps,
$\{\bar{Q}^g\}_{g\in\{\mathbb{G}^i\}_{i\in\mathbb{Q}^c}}$: nominal water flow for all controllable flows,
η: efficiencies matrix,
A: adjacency matrix,
$\underline{SoC}$, $\overline{SoC}$: reservoir lower and upper limits.
Output: $\{s_t^g\}_{g\in\{\mathbb{G}^i\}_{i\in\mathbb{Q}^c}}$: activation signal for all pumps,
$\{Q_{i,\tilde{T}(t)}\}_{i\in\mathbb{Q}^c}$: real-time estimation of the controllable flows,
$SoC_{\tilde{T}(t)}\}$: real-time estimation of the state of charge of all reservoirs
Solve:

$$\min \sum_{t\in\tilde{T}(t)} C\cdot(\Delta P_t^{up}+\Delta P_t^{down}) \tag{36}$$

s.t. $\forall t\in\tilde{T}(t)$:

$$\sum_{\forall i\in\mathbb{Q}^c} P_{i,t}+\hat{P}_t^{upc}-\hat{P}_t^{res}=\bar{P}_t^{DA}+\Delta P_t^{up}-\Delta P_t^{down} \tag{37}$$

$$P_{i,t}=\sum_{g\in\mathbb{G}^i} s_t^g\cdot\bar{P}^g,\quad \forall i\in\mathbb{Q}^c \tag{38}$$

$$Q_{i,t}=\sum_{g\in\mathbb{G}^i} s_t^g\cdot\bar{Q}^g,\quad \forall i\in\mathbb{Q}^c \tag{39}$$

$$SoC_{t+\Delta t}^r=SoC_t^r+\sum_{i\in\mathbb{Q}^u} a_{r,i}\cdot\eta_{r,i}\cdot\hat{Q}_{i,t}+\sum_{i\in\mathbb{Q}^c} a_{r,i}\cdot\eta_{r,i}\cdot Q_{i,t}\quad \forall r\in R \tag{40}$$

$$\underline{SoC}^r\le SoC_t^r\le\overline{SoC}^r,\quad \forall r\in R, \tag{41}$$

$$s_t^g-s_{t-1}^g=b_t^g-e_t^g,\forall g\in\mathbb{G}^i,\quad \forall i\in\mathbb{Q}^c \tag{42}$$

$$b_t^g+\sum_{t}^{t+k\cdot\Delta t} e_t^g\le 1,\forall g\in\mathbb{G}^i,\quad \forall i\in\mathbb{Q}^c \tag{43}$$

$$e_t^g+\sum_{t}^{t+m\cdot\Delta t} b_t^g\le 1,\forall g\in\mathbb{G}^i,\quad \forall i\in\mathbb{Q}^c \tag{44}$$

$$s_t^1\le s_t^2\le\cdots\le s_t^{|\mathbb{G}^i|},\quad \forall i\in\mathbb{Q}^c \tag{45}$$

$$s_t^g,b_t^g,e_t^g\in\{0,1\},\forall g\in\mathbb{G}^i,\quad \forall i\in\mathbb{Q}^c \tag{46}$$

$$\Delta P_t^{up},\Delta P_t^{down}\ge 0.,\quad \forall t\in\tilde{T}(t) \tag{47}$$

During this pilot project the station of Stembert was operated automatically by AMEO for a period of 16 days.

A. Reservoir operation

In this section, we will focus on the operation of the two large reservoirs, called Louveterie and Bronde, with $30,000m^3$ capacity each, as depicted in Figure 3a. Water from the treatment plant is gathered in a small reservoir called Cisternes with capacity $5,000m^3$. Water from this reservoir is treated and then pumped through five low-pressure pumps and into Bronde. Subsequently, four high-pressure water pumps are responsible for pumping water either towards Louveterie, or directly towards the water network. Each one of these high-pressure pumps, when operated, consumes 250kW and creates a flow of $1,000m^3/h$. Alternatively, water stored in Louveterie can be directed towards the water network that is supplying the area of Liège.

Conventionally, the operating strategy of both pump groups is based on thresholds of the water level in the reservoirs upstream and downstream. More precisely, when the water level of Bronde is between $2.8m$ and $4.2m$ one pump is operating. If the water level is higher than $4.2m$ then an additional pump starts operating in parallel. When the water level drops below $2.8m$ then the water pump towards Louveterie stops. Additionally, pumping water towards Louveterie is suspended in case the water level in Louveterie is higher than $4.78m$. The operating strategy of the low-pressure pumps responsible for pumping water from the Cisterns to Bronde is the following. When the water level of Cisterns is between $2.2m$ and $3.45m$ one pump is operating. If the water level is higher than $3.45m$ then two pumps are operating in parallel. When the water level drops below $2.2m$ then the water pump towards Bronde stops. Due to restrictions related to the chemical composition of the water gathered in the reservoir of Cisternes we assume that the WTS operator cannot change the conventional control strategy for the low-pressure pumps. These rule-based control strategies for the conventional operation of both pump groups together with the model of the station detailed in Section II-A are used to simulate the conventional operation and power consumption of the station during the 15-day period of the pilot phase.

In the following we consider that the WTS operator can benefit from its flexibility potential by adapting the operation of the high-pressure pump group $\mathbb{G}^3$ as illustrated in Figure 3b. The set of flows that appear in the selected system is $\mathbb{Q}=\{Q_1,Q_2,Q_3,Q_4,Q_5,Q_6,Q_7,Q_8\}$. Out of the set of all flows we distinguish between the controllable flows $\mathbb{Q}^c=\{Q_3\}$ and the uncontrollable ones $\mathbb{Q}^u=\{Q_1,Q_2,Q_4,Q_5,Q_6,Q_7,Q_8\}$. The controllable flow Q_3 is controlled by pump group that consists of 3 individual pumps, i.e. $\mathbb{G}^3=\{1,2\}$. Each of these pumps is able to generate a flow of $\bar{Q}^1,\bar{Q}^2=1000m^3/h$ and its power consumption is $\bar{P}^1,\bar{P}^2=250kW$.

There are two reservoirs involved in our study so we consider $R=\{Br,Lou\}$. The adjacency matrix used for this

case study is:

$$A = \begin{array}{c} \\ Brou \\ Lou \end{array} \begin{array}{c} \begin{array}{cccccccc} Q_1 & Q_2 & Q_3 & Q_4 & Q_5 & Q_6 & Q_7 & Q_8 \end{array} \\ \begin{bmatrix} 0 & 1 & -1 & 0 & -1 & -1 & 0 & 0 \\ 0 & 0 & 1 & -1 & 0 & 0 & 0 & 0 \end{bmatrix} \end{array}$$

The inflow to Bronde is $\mathbb{Q}^{Br,in} = \{Q_2\}$ and the outflows are $\mathbb{Q}^{Br,out} = \{Q_5, Q_6\}$. The considered reservoir security limits for Bronde are $\underline{SoC}^{Br} = 12,000m^3$, $\overline{SoC}^{Br} = 27,000m^3$. The inflow for Louveterie is $\mathbb{Q}^{Lou,in} = \{Q_3\}$ and the outflow is $\mathbb{Q}^{Lou,out} = \{Q_4\}$. The considered reservoir security limits for Louveterie are $\underline{SoC}^{Lou} = 15,000m^3$, $\overline{SoC}^{Lou} = 28,000m^3$.

B. System identification

As described in Section III-A, in order to have a working model of the WTS we need to identify the efficiencies of the input/output flows for each water reservoir (η). To this end, we use historical data of water flows and state of charge for each of the two reservoirs namely, Bronde and Louveterie. The average error achieved was $\sim$4%. The values of the obtained parameters are the following:

$$\eta = \begin{array}{c} \\ Brou \\ Lou \end{array} \begin{array}{c} \begin{array}{cccccccc} Q_1 & Q_2 & Q_3 & Q_4 & Q_5 & Q_6 & Q_7 & Q_8 \end{array} \\ \begin{bmatrix} 0 & 0.95 & 1 & 0 & 1.01 & 1.01 & 0 & 0 \\ 0 & 0 & 0.96 & 1.05 & 0 & 0 & 0 & 0 \end{bmatrix} \end{array}$$

C. Producing forecasts

In this section, we present the results for the generation of forecasts that are used in the day-ahead nomination and the real-time control decision processes. It is important to note that, there was no RES production considered during the period of the pilot project. For the day-ahead nomination step we need to predict the day-ahead prices in order to optimize the WTS consumption pattern. As described in Section III-B, we use an instance of *Facebook prophet*. The day-ahead optimization horizon is selected to be $N = 2$ days. It is important to note, that accuracy in terms of absolute values is not the main goal at this step. Instead, a forecaster that can predict well the shape of the day-ahead price curve, i.e. the periods of low and high prices, is sufficient for producing an optimal day-ahead nomination.

Additionally, as described above, in both the day-ahead and the real-time stage we need to produce forecasts for the uncontrollable flows ($\mathbb{Q}^u = \{Q_1, Q_2, Q_4, Q_5, Q_6\}$) of the system presented in Figure 3b. Out of the set of uncontrollable flows, during the exploratory data analysis there were two flows, namely Q_4 (Adduction) and Q_5 (Restitution) that were categorised to have strong daily seasonality. For each one of these two flows we use a *Facebook prophet* instance.

The rest of the uncontrollable flows do not have some daily seasonality and mainly depend on the cleaning processes of the filters (Lavage). In order to obtain a forecast for flows $\{Q_1, Q_2, Q_6, Q_7, Q_8\}$ we work as following. For the prediction of the inflow to the Bronde Q_2 and the flow from the Bronde to Lavage Q_6, we need to simulate the conventional operation for the part of the station that we do not control i.e. upstream of the low-pressure pumps. First, we predict based on historical data the water consumption for Lavage $\hat{Q}_8$ and the inflow rate at Cisterns $\hat{Q}_0$. Next, we simulate the state of charge of Cisterns using the pumping strategy described in Section IV-A, as presented in Algorithm 3, in order to predict the flow $\hat{Q}_1$.

Algorithm 3: Rule-based control of Cisterns.

Inputs: $\hat{Q}_{0,t}$, $\hat{SoC}_t^{Cis}$
if $2.2m < \hat{SoC}_t^{Cis} < 3.45m$ **then**
  $\hat{Q}_{1,t} \leftarrow 1000m^3$
else if $3.45m < \hat{SoC}_t^{Cis}$ **then**
  $\hat{Q}_{1,t} \leftarrow 2000m^3$
else
  $\hat{Q}_{1,t} \leftarrow 0m^3$
end if
Output: $\hat{Q}_{1,t}$

Algorithm 4: Rule-based water-flow prediction.

Inputs: $\hat{Q}_{1,t}, \hat{Q}_{8,t}$
if $\hat{Q}_{8,t} > 0$ **then**
  if $\hat{Q}_{8,t} > \hat{Q}_{1,t}$ **then**
    $\hat{Q}_{2,t} \leftarrow 0$
    $\hat{Q}_{6,t} \leftarrow \hat{Q}_{8,t} - \hat{Q}_{1,t}$
    $\hat{Q}_{7,t} \leftarrow \hat{Q}_{1,t}$
  else
    $\hat{Q}_{2,t} \leftarrow 0$
    $\hat{Q}_{6,t} \leftarrow 0$
    $\hat{Q}_{7,t} \leftarrow \hat{Q}_{1,t}$
  end if
else
  $\hat{Q}_{2,t} \leftarrow \hat{Q}_{1,t}$
  $\hat{Q}_{6,t} \leftarrow 0$
  $\hat{Q}_{7,t} \leftarrow 0$
end if
Output: $\hat{Q}_{2,t}, \hat{Q}_{6,t}, \hat{Q}_{7,t}$

The predictions of the water flows $\hat{Q}_1$ and $\hat{Q}_8$ serve as input to the rule-based algorithm presented in Algorithm 4, in order to predict flows $\hat{Q}_{2,t}, \hat{Q}_{6,t}, \hat{Q}_{7,t}$. In case that, we predicted that at timestep t the filters are being washed ($\hat{Q}_{8,t} > 0$), then flow $\hat{Q}_{1,t}$ is used entirely for this purpose, i.e. $\hat{Q}_{2,t} = 0$ and $\hat{Q}_{7,t} = \hat{Q}_{1,t}$. If the water flow needed for filter cleaning Q_8 is larger than the water flow $\hat{Q}_{1,t}$ (i.e. $\hat{Q}_{8,t} > \hat{Q}_{1,t}$), additional water flows from Bronde $\hat{Q}_{7,t} = \hat{Q}_{8,t} - \hat{Q}_{1,t}$. In the case that, there is no water needed for filter cleaning we have $\hat{Q}_{2,t} = \hat{Q}_{1,t}$.

D. Day-ahead nomination & Real-time control

As described in Section III, the WTS operator makes two decision steps in order to valorize its flexibility in the short-term market. The first step takes place one day in advance by nominating the WTS consumption plan for the next day.

This article has been accepted for publication in IEEE Transactions on Smart Grid. This is the author's version which has not been fully edited and content may change prior to final publication. Citation information: DOI 10.1109/TSG.2023.3272469

TABLE I: Cost reduction in Stembert water treatment station in the pilot 15-days period.

	Conventional	Flexible	Reduction
High-pressure pumps cost (€)	22,614	20,195	10.7%
Pumping cost (€)	51,667	48,182	6.7%
Total cost (€)	97,385	93,900	3.6%

The second step takes place in real-time and it consists in matching the day-ahead plan to the real-time consumption. The day-ahead plan (orange) and the real-time value (blue) of the power consumed by the high-pressure pumps is presented in Figure 4a. It can be observed that, there are really minor differences between the two which indicates that the WTS can be securely operated based on the day-ahead plan with minor corrections necessary in real-time.

In effect, small deviations (errors) between day-ahead flow predictions and realisations can be dampened due to the reservoirs and in particular the one of Bronde. This can be observed by the day-ahead estimation (orange) versus the real-time operation (blue) of the state of charge (i.e. water volume) of Bronde illustrated in Figure 4b. We can see that while the shapes of the two curves are very similar there are discrepancies that are attributed to the imperfect forecasts of water flows that enter and leave Bronde ($\{Q_1, Q_5, Q_6\}$). As can be seen in Figure 4f the seasonal flow of Restitution (Q_2) can be predicted with high accuracy.

On the other hand, as it can be observed in Figure 4c, the day-ahead estimation (orange) versus the real-time operation (blue) of the state of charge of Louveterie are practically identical. This occurs due to the fact that the predictions related to the water demand (Q_4) are quite accurate, as it can be seen in Figure 4e and the pumping is exactly the same as the day-ahead pumping plan. Finally, we can see in Figure 4d that the day-ahead price forecast is able to successfully capture the peak versus off-peak periods of the day.

The flexible consumption of the Stembert WTS during the pilot project versus the previous non-flexible consumption is illustrated in Figure 5a. More precisely, we can see clearly in Figure 5b that part of the consumption related to the controllable high-pressure pumps is shifted from periods of the day with high prices to periods where the price is low. The cost reduction achieved during the 15-days period of the project is presented in Table I. We can see a substantial cost reduction ($\sim$11%) on the cost related to the operation of the high-pressure pumps and 6.7% cost reduction considering all pumping processes. This reduction is related to the fact that the changes in the operation of the high-pressure pump may affect indirectly the pumping process in the low-pressure pumping group. Finally, a 3.6% was achieved when taking into account the total consumption of the WTS.

V. Conclusions

Flexibility is key for enabling the large-scale penetration of RES in the context of the energy transition. In this paper, we exploit the value of flexibility coming from water treatment stations. We present a generic modelling framework for the

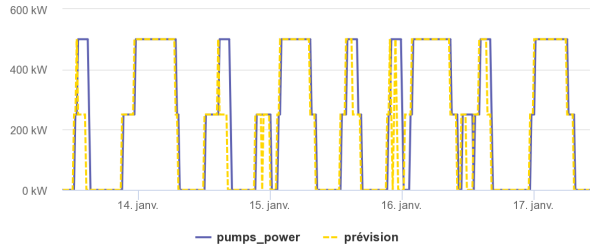

(a) Day-ahead (orange) nomination versus the real-time operation (blue) of the controllable high-pressure pumps.

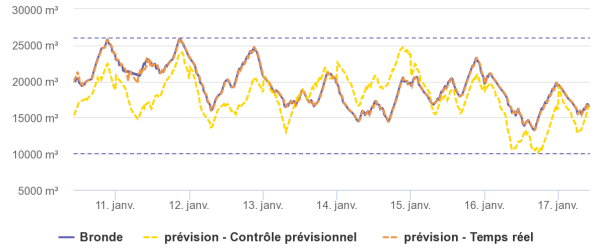

(b) Day-ahead estimation (orange) versus the real-time operation (blue) of the state of charge (i.e. water volume) of Bronde.

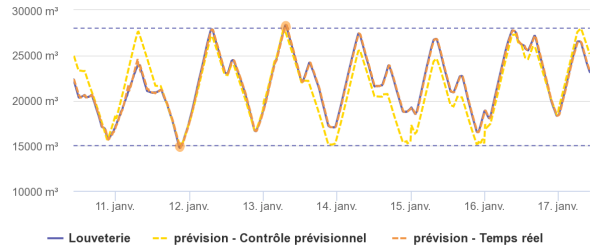

(c) Day-ahead estimation (orange) versus the real-time operation (blue) of the state of charge (i.e. water volume) of Louveterie.

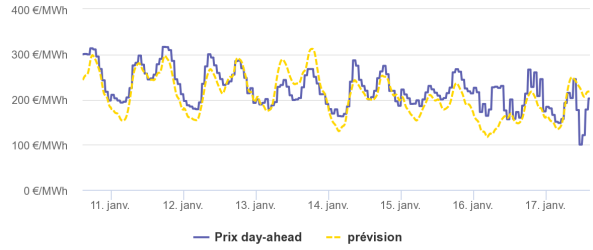

(d) Day-ahead price forecast (orange) versus the realisation (blue).

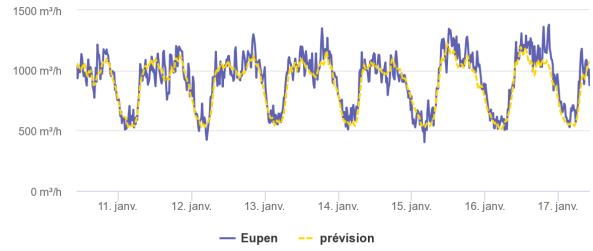

(e) Day-ahead forecast of flow Q_4 (orange) versus the realisation (blue).

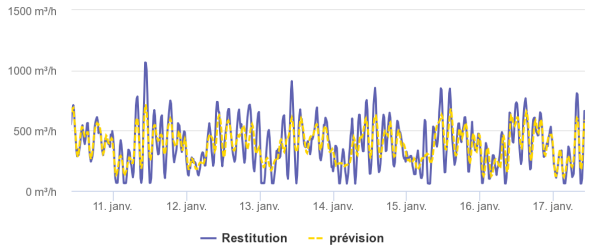

(f) Day-ahead forecast of flow Q_2 (orange) versus the realisation (blue).

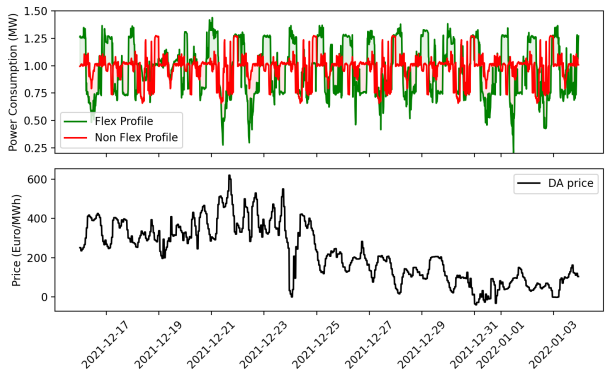

(a)

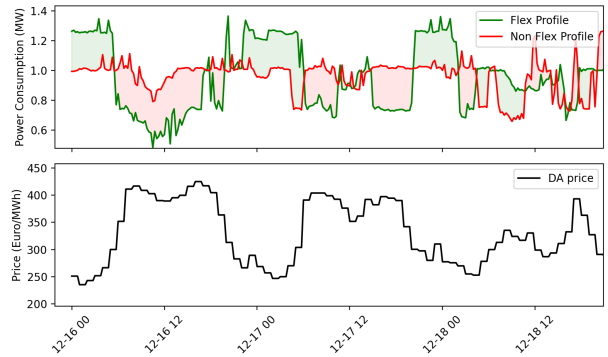

(b)

Fig. 5: The flexible consumption of the Stembert WTS during the pilot project versus the conventional non-flexible consumption during the pilot phase.

energy market participation and the real-time operation of a WTS. We apply this framework to a real-life pilot project in Wallonia, where the operation of a WTS has been adapted and consumption from the high-consuming pumping processes is shifted during the day. The results from the pilot project indicate cost reduction up to 11% and a large potential for flexible WTS.

Acknowledgements

The authors would like to thank Mr. Avelino Gonzalez and Mr. Thierry Hoebeke for the fruitful discussions regarding the operation of the Stembert water treatment station.

References

[1] (2019) Paris agreement. [Online]. Available: https://unfccc.int/process-and-meetings/the-paris-agreement/the-paris-agreement

[2] E. Commission. (2019) Clean energy for all europeans. [Online]. Available: https://op.europa.eu/en/publication-detail/-/publication/b4e46873-7528-11e9-9f05-01aa75ed71a1

[3] A. Ulbig and G. Andersson, "On operational flexibility in power systems," in *2012 IEEE Power and Energy Society General Meeting*, 2012, pp. 1–8.

[4] H. Chandler, *A Guide to the Balancing Challenge*, 2011. [Online]. Available: www.iea.org

[5] V. Rious, Y. Perez, and F. Roques, "Which electricity market design to encourage the development of demand response?" *Economic Analysis and Policy*, vol. 48, pp. 128–138, 2015.

[6] R. Sharifi, S. Fathi, and V. Vahidinasab, "A review on demand-side tools in electricity market," *Renewable and Sustainable Energy Reviews*, vol. 72, pp. 565–572, 2017. [Online]. Available: https://www.sciencedirect.com/science/article/pii/S1364032117300230

[7] M. Parvania, M. Fotuhi-Firuzabad, and M. Shahidehpour, "Optimal demand response aggregation in wholesale electricity markets," *IEEE Transactions on Smart Grid*, vol. 4, pp. 1957–1965, 12 2013.

[8] S. Vandael, B. Claessens, D. Ernst, T. Holvoet, and G. Deconinck, "Reinforcement learning of heuristic ev fleet charging in a day-ahead electricity market," *IEEE Transactions on Smart Grid*, vol. 6, no. 4, pp. 1795–1805, 2015.

[9] Z. Xu, Z. Hu, Y. Song, and J. Wang, "Risk-averse optimal bidding strategy for demand-side resource aggregators in day-ahead electricity markets under uncertainty," *IEEE Transactions on Smart Grid*, vol. 8, no. 1, pp. 96–105, 2017.

[10] C. Utama, S. Troitzsch, and J. Thakur, "Demand-side flexibility and demand-side bidding for flexible loads in air-conditioned buildings," *Applied Energy*, vol. 285, p. 116418, 2021. [Online]. Available: https://www.sciencedirect.com/science/article/pii/S0306261920317815

[11] B. Zimmermann, H. Gardian, and K. Rohrig, "Cost-optimal flexibilization of drinking water pumping and treatment plants," *Water*, vol. 10, no. 7, 2018. [Online]. Available: https://www.mdpi.com/2073-4441/10/7/857

[12] A. Zohrabian, S. L. Plata, D. M. Kim, A. E. Childress, and K. T. Sanders, "Leveraging the water-energy nexus to derive benefits for the electric grid through demand-side management in the water supply and wastewater sectors," *Wiley Interdisciplinary Reviews: Water*, vol. 8, no. 3, p. e1510, 2021.

[13] D. Fooladivanda, A. D. Domínguez-García, and P. W. Sauer, "Utilization of water supply networks for harvesting renewable energy," *IEEE Transactions on Control of Network Systems*, vol. 6, no. 2, pp. 763–774, 2019.

[14] M. K. Singh and V. Kekatos, "Optimal scheduling of water distribution systems," *IEEE Transactions on Control of Network Systems*, vol. 7, no. 2, pp. 711–723, 2020.

[15] K. Oikonomou, M. Parvania, and R. Khatami, "Optimal demand response scheduling for water distribution systems," *IEEE Transactions on Industrial Informatics*, vol. PP, pp. 1–1, 02 2018.

[16] A. Stuhlmacher and J. L. Mathieu, "Flexible drinking water pumping to provide multiple grid services," *Electric Power Systems Research*, vol. 212, p. 108491, 2022. [Online]. Available: https://www.sciencedirect.com/science/article/pii/S0378779622005806

[17] C. Mkireb, A. Dembélé, A. Jouglet, and T. Denoeux, "Robust optimization of demand response power bids for drinking water systems," *Applied Energy*, vol. 238, pp. 1036–1047, 2019. [Online]. Available: https://www.sciencedirect.com/science/article/pii/S0306261919301461

[18] A. Stuhlmacher and J. L. Mathieu, "Chance-constrained water pumping to manage water and power demand uncertainty in distribution networks," *Proceedings of the IEEE*, vol. 108, no. 9, pp. 1640–1655, 2020.

[19] E. Sarmas, E. Spiliotis, V. Marinakis, G. Tzanes, J. K. Kaldellis, and H. Doukas, "Ml-based energy management of water pumping systems for the application of peak shaving in small-scale islands," *Sustainable Cities and Society*, vol. 82, p. 103873, 2022.

[20] S. J. Taylor and B. Letham, "Forecasting at scale," *The American Statistician*, vol. 72, no. 1, pp. 37–45, 2018.